Ultraviolet light induced single step all-optical poling in lithium niobate

C. L. Sones, A. C. Muir, S. Mailis and R. W. Eason

Optoelectronics Research Centre, University of Southampton, Highfield, Southampton, S017 1EN, UK

Main contact email address	cls@orc.soton.ac.uk

Introduction

Precision-scale engineering of domains in ferroelectric lithium niobate crystals is a subject of extensive research recently due to the numerous applications that this material has in optical telecommunications, nonlinear optics and optical sensing. The fabrication of well-defined periodic domain structures for this range of applications requires a robust method for ferroelectric domain inversion which can achieve the desired spatial ferroelectric domain distributions even on submicron scales. Furthermore, this method must be flexible, repeatable, and easy to apply.

So far the most popular method for ferroelectric domain reversal, referred to as E-field poling, involves the application of an external electric field across the two opposite z faces of the crystal at room temperature. Spatially selective ferroelectric domain reversal is achieved by covering one z face with photolithographically patterned photoresist or metal which provides the necessary spatially selective electric field contrast. However, the electric field contrast provided by the patterned photoresist is rather poor and consequently widths of ferroelectric domain produced by this method are limited to greater than a few microns.

We have directed considerable effort to the end goal of establishing a simple and reliable domain inversion technique that can circumvent the limitations of simple E-field poling. We have been experimenting with two different light-induced ferroelectric domain engineering approaches which we refer to as all-optical poling[1] (AOP) and light-assisted electric field poling[2] (LAP). The main feature in both methods is that the E-field contrast provided by the presence of patterned electrodes is now no longer necessary. The AOP approach attempts to achieve the required control over the formation of micron and submicron scale periodic domains via the use of a patterned optical field instead of the patterned electric field in the conventional technique of E-field poling. The LAP approach is a modified E-field poling technique wherein domain inversion is achieved under the combined influence of a patterned optical field and an un-patterned E-field. In this method the simultaneous presence of light results in a reduction of the field required to achieve domain inversion in the crystal, and hence eases the requirement of an otherwise extremely high electric field (~22 kV mm^{-1}) for conventional domain inversion.

Several groups have also studied the interaction between illuminating laser light and ferroelectric crystals, using c.w. light at different wavelengths (305 & 334 nm[3], 514 nm[4]) for domain inversion in undoped lithium niobate. Domain patterning in MgO-doped lithium niobate crystals using ultraviolet light from a Hg-lamp has also been reported. [5] Our earlier LAP experiments have demonstrated light-controlled micron scale domain patterning in congruent and MgO-doped single crystal material through an interaction with c.w. and pulsed laser light. We have reported an order-of-magnitude reduction in the electric field required for domain nucleation in lithium niobate crystals induced by illumination from a focused c.w. laser beam at wavelengths of 514, 488 and 457 nm. [2] We have also observed reduction in the nucleation field via use of ultra-short laser pulses (~120-150 fs) of near-ultraviolet (305 nm) to near-infrared (800 nm) wavelengths. [6]

Our AOP experiments conducted at the LSF in RAL and also at the ORC with the NSL-4/5 lasers using a ns UV (298-329 nm) light have also resulted in submicron AOP surface domains. [1,7] We have been exploring other wavelengths which are highly absorbed by the crystal with an end goal of pushing the AOP domain further in the crystal, and possibly achieving better control on the growth and the formation of the AOP domains. This has been possible with the CWL1 continous wave (c.w) frequency-doubled argon-ion laser from CLF-RAL laser loan pool that provides a wavelength range of 229-264 nm.

Our recent studies using this c.w source have interestingly revealed that AOP is achievable even without the high peak intensities, previously assumed essential, of a pulsed source. Some of the initial results from these experiments are described here later.

Experiments and results

The experimental set-up involved a 5 cm focal length lens that focused a spatially-filtered and collimated beam from the frequency doubled Ar-ion laser on the z face of the z-cut undoped congruent lithium niobate crystals. The beam was focused to a measured spot diameter of ~5 μm. The selected incident laser wavelength was 244 nm, at which the lithium niobate crystals are known to be highly absorbing. The incident power was varied from 20-28 mW, yielding an intensity range of 125-175 kW cm^{-2}.

The crystals used in the study were 0.5 mm thick, optically polished z-cut, undoped congruent lithium niobate wafers supplied by Crystal Technology, USA.

The crystals were mounted on motorised translational stages which not only allowed for the precise positioning of the illuminated z face at the point of focus, but also allowed for the motion of the illuminated z faces along the two directions lateral to the incident beam. Crystal faces were illuminated either by translating the stage at a uniform speed relative to the static incident beam, or just leaving it stationary, thereby inscribing structures in the shape of straight lines or circular dots.

Lines were drawn on the z faces of the crystals along the crystallographic x or y directions by moving the stages at speeds ranging from 0.05-0.3 mm s^1. A range of different speeds was tried to observe its effect on the widths and the depths of the directly written domain structures.
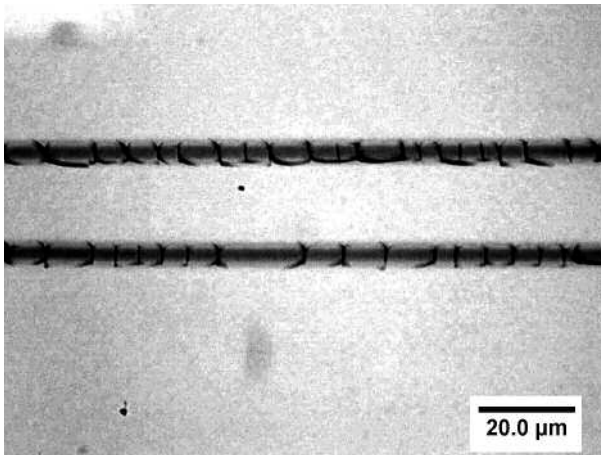
Figure 1. Unetched UV exposed + z face, showing line scanned at incident power 30 mW and scan speed 50 μm s⁻¹. Two distinct features can clearly be seen; a central darkened region and a wider surface damaged region.

Figure 2. Plot showing variations of the widths of the total affected regions and (asterix) and central darkened (triangle) regions of the UV exposed lines.

For static exposures, (when the stages were not moving), the total time for which a particular position on the crystal face is illuminated was controlled using a shutter positioned along the path of the beam. The set of different exposure times ranging from a few milliseconds to one second were investigated to study the effect of the illumination time on the formation of the domain features. For a particular exposure time, an array of illuminated spots was formed by successively illuminating several equidistant positions on the crystal face. The separation between the edges of adjacent illuminated spots in the arrays varied from a few microns to zero microns. This permitted us to verify whether the proximity effect observed in pulsed AOP, (which forbids the merging of isolated domains with those in their near proximity, and hence prevents the formation of continuously joined domains), would also be an obstacle in the c.w AOP case.

Each of the explored illumination conditions was duplicated for a set of complementary z faces, thus allowing for a direct comparison of the AOP effect on each of those faces.

Initial examination of the illuminated faces was performed with an optical microscope between cross polarisers. Routinely employed domain visualisation techniques of wet chemical etching (in HF acid), and Piezorespsonse Force microscopy (PFM) were used for establishing the domain nature of directly written structures. Further measurements and characterisation of the domain inverted structures was done with a surface profiler and scanning electron microscope (SEM).

Initial examination of the UV scanned lines using a microscope revealed that in the case of both faces, lines written at higher powers (above 24 mW) and slower speeds result in damaged surfaces. The lines were seen to be composed of two distinct regions; a central region where the crystal is seen to undergo some darkening, and an outer lighter region with cracks resulting from thermal deformations and melting along its lengths. In all these lines the widths of the darkened regions (ranging from 1.4-2.5 μm) were significantly less than the $1/e^2$ beam diameter of 5 μm. A high magnification optical microscope image of Fig. 1 shows the extent of damage on the illuminated
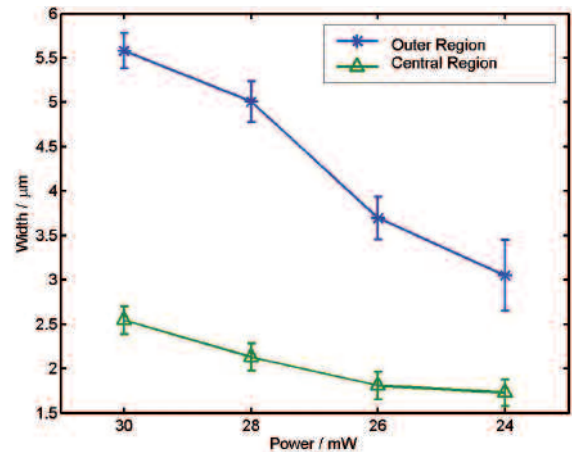
surfaces, and also clearly shows the two distinct affected regions. Surfaces of lines scanned at lower powers however appeared smooth and free of any of the randomly orientated cracks and voids associated with lines written at higher powers. The surface topography of these lines studied using a surface profiler confirm the absence of surface damage. A preliminary study of the variation in the widths of the scanned lines revealed a dependence on the writing/scanning conditions, namely the incident power/intensity and the scan speeds, with the larger widths corresponding to lines scanned at higher powers and or slower speeds. The measured widths of the total affected regions agree with those predicted by our previous thermal model[8]. Fig. 2 shows the width variation of affected regions with power for a set of lines scanned at identical speeds.

After the initial assessment the samples were studied using a PFM to determine if domain inversion had occurred in the illuminated regions. Fig. 3a, b show piezoresponse images of lines scanned on either of the z faces, with the dark lines in the image corresponding to the UV written lines. Interestingly, the contrast in the acquired PFM images for the scanned lines, improved with the incident power, which points to a difference in depth of the affected region. After a first set of PFM measurements, samples were annealed at 200˚C for 4 hours to eliminate the traces of residual charge, if any, from the illumination. The second set of measurements after the annealing step did not produce any change in the observed contrast of the piezoresponse images, which then verifies the piezoelectric nature of the domain inverted lines.

Moreover as shown in Fig. 3c a fortuitous accident with the tuning of the writing stages has also shown that the creation of the domains is not hindered by the imposed symmetry of the crystal (as in case of conventional poling techniques where domains will preferentially grow along the x or y axes of the crystal) but that domains can be created with arbitrary shape.

The samples were finally etched in pure HF acid to ascertain their domain nature via the established z face differential etch mechanism, which is know to selectively etch on the - z faces of lithium niobate. The samples were first briefly etched for a period of 5mins to determine the
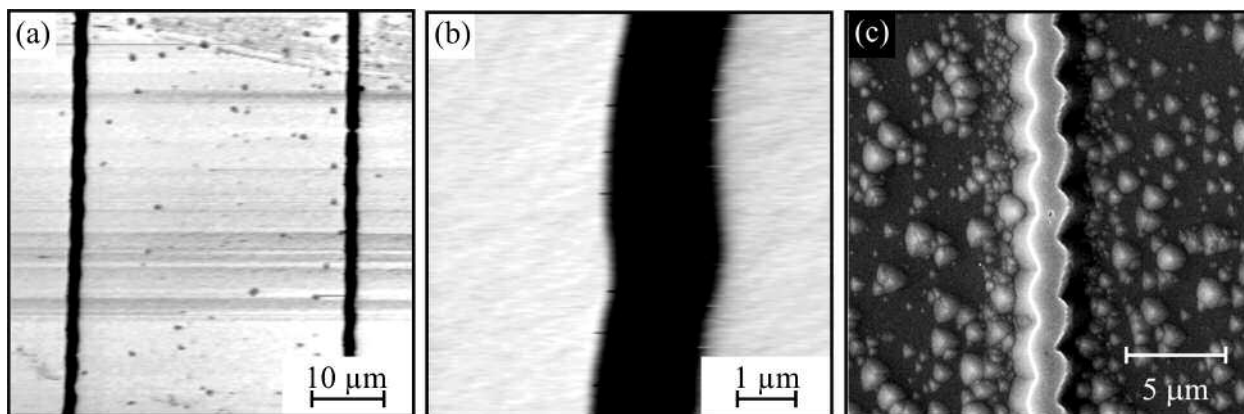
Figure 3. a, b) PFM images of written lines. c) SEM image showing a similar domain inverted line after etching.

profile of the etched domain inverted scanned lines. Etched structures with complementary shapes were observed for the two *z* faces, namely domain inverted lines on the + *z* face revealed etched trenches, whereas a similarly inverted lines on the – *z* face were etched out to reveal surface relief ridges. The samples were further etched (in steps of 5 min for about an hour), and subsequently imaged and profiled in order to determine the depths of the inverted domains. The shallow depths of the domain inverted regions were obvious from the scanning electron microscope (SEM) images seen in Fig. 4. Fig. 4a shows an SEM micrograph of an etched domain inverted trench formed on a + *z* face. Fig. 4b shows a SEM micrograph of an etched domain inverted ridge (revealed on an etched - *z* face). The gradients of the upper and lower edges of the ridge structure in Fig 4b, provides further evidence of its domain inverted nature. The upper edge of the ridge does not display any side etching whilst the lower surface displays a shallow gradient indicating side etching. Inversion of the *z* axis also results in the inversion of the *y* axis, and the differential etching mechanism of the *y* faces then results in these differing gradients. This has also been observed on domain structures written on - *y* faces through the differential etching behaviour of the *z* faces. Fig 5 shows an SEM micrograph of etched domain inverted ridges (revealed on an etched - *z* face) imaged from their sides at an angle of 49˚. The thin film like layer with a thickness of ~ 1µm, suspended above the pyramid like structures observed on etched - *z* faces, corresponds to the UV induced domain inverted layer.

Conclusions

In summary we have demonstrated AOP via use of a c.w. light at 244 nm from a frequency doubled Ar-ion laser (CWL-1) on loan from the CLF-RAL. Domain inversion
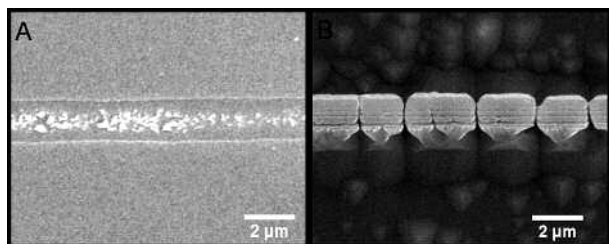

Figure 4. a. SEM image of an etched - z domain on a + z face. Incident power was 20 mW, and scan speed was 50 µm s⁻¹. b. SEM image of an etched + z domain on a - z face. Incident power was 26 mW and scan speed was 50 µm s⁻¹.
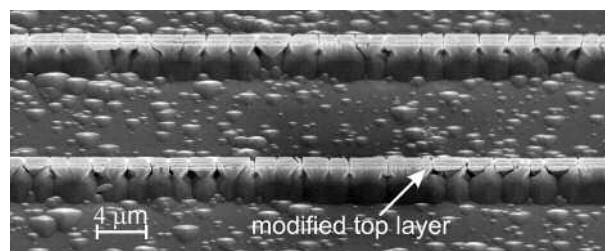

Figure 5. SEM image of an etched + z domain on a - z face. Incident power was 26 mW, and scan speed was 50 µm s⁻¹. Stage tilted by 49° to view sides of etched ridges.

was achieved for illumination on both the *z*-faces. The domain inverted regions, had widths comparatively smaller than those of the scanning laser beam, implying the possibility of sub-micron domain formation. The shapes of the inverted regions strictly adhered to those of the incident beam, which meant that it is possible to fabricate domains with arbitrary shape. The depths of the inverted domains are not quite those desired for guided wave interaction, however, we are confident that simple, post illumination processing can increase the domain depth whilst retaining the advantages of a direct-write system. In conclusion c.w AOP presents a single step versatile approach to domain inversion in lithium niobate.

References

1. C. E. Valdivia, C. L. Sones, J. G. Scott *et al., Applied Physics Letters* **86** (2), 022906 (2005).
2. C. L. Sones, M. C. Wengler, C. E. Valdivia *et al., Applied Physics Letters* **86** (21), 212901 (2005).
3. M. Muller, E. Soergel, and K. Buse, *Applied Physics Letters* **83** (9), 1824 (2003).
4. V. Dierolf and C. Sandmann, *Applied Physics Letters* **84** (20), 3987 (2004).
5. A. Fujimura, T. Sohmura, and T. Suhara, *Electronics Letters* **39** (9), 719 (2003).
6. C. E. Valdivia, C. L. Sones, S. Mailis *et al.,* in *ISDS* (Ekaterinburg Russia, 2005).
7. I. T. Wellington, C. E. Valdivia, T. J. Sono *et al., Applied Surface Science* **253** (9), 4215 (2007).
8. A.C. Muir, G. J. Daniell, C. P. Please *et al., Applied Physics A-Materials Science & Processing* **83** (3), 389 (2006).